iomac
International Operational Modal Analysis Conference

11th International Operational Modal Analysis Conference

20 - 23 May 2025 | Rennes, France

Dynamic Characterization of a Flexible Wing Model Using Stochastic Modal Appropriation for Nonlinear Aeroelastic Analysis

Daniele Antonini [1], *Gianpietro Fronteddu* [2], , *Roberto Giovanni Sbarra* [2], , *Ludovica Onofri* [2], , *Giuliano Coppotelli* [2], , *Maher Abdelgani* [3]

[1] University of Rome "La Sapienza", Dipartimento di Ingegneria Meccanica e Aerospaziale, Via Eudossiana, 18, 00184, Rome, Italy, daniele.antonini@uniroma1.it

[2] University of Rome "La Sapienza", Dipartimento di Ingegneria Meccanica e Aerospaziale, Via Eudossiana, 18, 00184, Rome, Italy

[3] Department of Mechanical Engineering, City Taffala, University of Sousse, Higher Institute of Applied Sciences and Technology of Sousse, 4003 Sousse, Tunisia

ABSTRACT

In modern aerospace engineering, the push for lightweight and flexible wings aims to enhance efficiency, reduce fuel consumption, and enable adaptation to extreme flight conditions. These flexible structures undergo large deformations, highlighting a need for validated nonlinear numerical models, making Operational Modal Analysis (OMA) essential for dynamic characterization in environmental conditions. This study applies the Stochastic Modal Appropriation (SMA) method to a flexible wing model inspired by the Pazy Wing, built and tested at the University of Rome "La Sapienza". SMA estimates modal parameters using the correlation function as an impulse response under white noise excitation. The goal is to demonstrate the effectiveness of the SMA method even when natural frequencies are closely spaced, as observed in the Pazy wing. The method effectively captures the flutter mechanism, characterized by a hump mode where the first torsional frequency approaches the second bending mode. However, compared to other MDOF OMA techniques, SMA shows discrepancies, particularly in damping estimation.

Keywords: Structure dynamics, Flexible Wing, Operational Modal Analysis, Stochastic Modal Appropriation

1. INTRODUCTION

High fuel efficiency and reduced emissions represent fundamental objectives in modern aircraft design. Consequently, the significance of lightweight structures is expected to become even more prominent in the future. From an aerodynamic perspective, high-aspect-ratio, slender wings are preferred as they minimize induced drag, thereby enhancing lift-to-drag ratios and extending operational range, Ref. [1]. In highly flexible wing configurations, the structure exhibits greater susceptibility to large deflections under the same operating conditions, influencing its dynamic response (modal properties) and, consequently, its aeroelastic behavior. The amplification of aeroelastic phenomena has the potential to compromise the adequacy of conventional aeroelastic models for the purpose of accurate predictions. A significant effort has been dedicated within the aeroelastic community to the development and implementation of high fidelity models, in both structural and aerodynamic domains, to accurately capture the aeroelastic behavior of flexible configurations across a wide range of flight conditions, Ref. [2]. The development of structural models for highly flexible wings requires accurate predictions of large deformations. Validation through wind tunnel tests or flight experiments is crucial to assessing model reliability and exploring nonlinear aeroelastic phenomena beyond current theories. However, due to the complexity of such tests, benchmark datasets for highly flexible wings remain limited [3–5]. The Large Deflection Working Group within the Aeroelastic Prediction Workshop, Ref. [6], represents a recent collaborative initiative aimed at investigating modeling challenges and experimental issues associated with highly flexible wings. In the third edition of this workshop, the selected test case was the Pazy wing, a highly flexible wing model specifically designed to study aeroelastic phenomena arising from large deformations, Ref. [7]. The Pazy wing undergoes large deformations, reaching up to 50% of its span under aerodynamic loading. Wind tunnel tests reveal multiple flutter mechanisms, primarily bending-torsion flutter, driven by the coupling of the second bending and first torsional modes. This coupling, influenced by static bending and dynamic pressure, leads to flutter appearing as a hump mode. The authors conducted an experimental campaign using the same wing model in different wind tunnel facilities to investigate its aeroelastic behavior. This experimental campaign aims to contribute to enriching the experimental database necessary for the development of predictive numerical models. Indeed, these data can support the construction of high-fidelity digital twins of highly flexible wings, enabling improved aeroelastic analysis and control in future aircraft design. The data collected were analyzed through Operational Modal Analysis (OMA), allowing for the identification of modal parameters and the assessment of dynamic characteristics. The results demonstrated a good agreement with existing literature, Ref. [8–10]. OMA techniques operate under the assumption of broadband excitation, such as white noise, within the frequency range of interest and leverage both time-domain and frequency-domain data. Modal parameters are extracted from the Power Spectral Density matrix using approaches such as Frequency Domain Decomposition and Hilbert Transform methods, Ref. [11, 12], or from correlation functions of the time responses as employed in Stochastic Subspace Identification-based methods, Ref. [13], and Ibrahim Time Domain, Ref.[14]. In the studies conducted by the authors, OMA techniques were applied to acceleration responses recorded during wind tunnel experiments to estimate modal parameters across different test conditions, defined by various combinations of wind tunnel velocity and wing model angle of attack. Given their capability to accurately identify these modal parameters, OMA methods enable the evaluation of their effectiveness in tracking the evolution of aeroelastic characteristics under varying operational conditions.

Various OMA techniques have been investigated in the literature, employing different identification strategies to estimate modal parameters in aeroelastic applications [15]. In this study, the Stochastic Modal Appropriation (SMA) method is proposed for the identification of the modal parameters of the Pazy wing model under its operating conditions. Originally developed in the time domain for Single Degree of Freedom (SDOF) systems, the SMA method enabled the estimation of natural frequencies and damping ratios by analyzing output correlations from random excitations. Its application to aeroelastic problems is particularly valuable from an operational standpoint, as it allows for system identification under real operating conditions while offering practical advantages over other methods, such as reduced sensitivity to harmonic components that may be blended with the random excitations when considering rotating structures as helicopters and ease of automation. The method proved to be effective for systems

with well-separated natural frequencies and light damping, enabling accurate modal characterization from stochastic data [16, 17].
This work is structured into five key sections, covering the SMA algorithm, the proposed innovation, and a numerical study to validate the method's robustness, ultimately applying it to experimental data from the Pazy wing campaign.

2. THEORETICAL BACKGROUND

2.1. SMA basic formulation

Building upon the formulation for a single-degree-of-freedom system, Ref. [18], the SMA method can also be applied to measure the dynamic response of a multi-degree-of-freedom (MDOF) system which exhibits behavior characterized by multiple damped harmonic responses within the bandwidth of interest. Let us consider a generic Multiple Input-Multiple Output (MIMO) system, defined by M mode shapes within the frequency range of interest. The system is subjected to random excitation at N_i input locations, while the time responses are measured at N_o output locations. The $N_o \times N_o$ cross-correlation matrix of the output responses is given by:

$$R(t) = \begin{bmatrix} R_{y_1 y_1}(t) & \cdots & R_{y_1 y_{N_0}}(t) \\ \vdots & \ddots & \vdots \\ R_{y_{N_0} y_1}(t) & \cdots & R_{y_{N_0} y_{N_0}}(t) \end{bmatrix} \tag{1}$$

The Power Spectral Density (PSD), defined as the Fourier transform of the autocorrelation function of the time series (corresponding to the diagonal terms in Eq. 1), provides a means to identify the expected natural frequencies of the system. This information underpins the application of the SMA method, which assumes a Single Degree of Freedom (SDOF) behavior characterized by a single damped harmonic response. This assumption holds when the natural frequencies are well separated and the system's modes exhibit light damping, ensuring that each mode remains distinct and its dynamic is governed by a single dominant harmonic component.
By filtering the time series in the neighborhood of a natural frequency, the system's dynamic correlation function for the ij-th entry of Eq. 1, representing the correlation between response signals i and j, can be expressed as:

$$R_{ij}(t) = {}_r c_{ij} e^{-\zeta_r \omega_r t} \left(\cos(\omega_d t) + \frac{\zeta_r}{\sqrt{1-\zeta_r^2}} \sin(\omega_d t) \right) \tag{2}$$

In this context, ω_d, ω_r, and ζ_r correspond to the r-th damped natural frequency, natural frequency, and damping ratio, respectively. The term ${}_r c_{ij}$ represents the contribution of the r-th mode to the displacement at the i-th degree of freedom (DOF) when the structure is subjected to excitation at the j-th DOF.
As part of the SMA method, Ref. [17], a mode-specific stretching and rotating parameter α_r is introduced for each mode. This parameter modifies the correlation sequence as $H(t) = R(t)(1 + j\alpha_r)$. The resulting correlation function is then convolved with a harmonic excitation at the driving frequency ω_r. The phase shift $\vartheta(\alpha_r, \omega_r)$ between the generic output response and the harmonic input excitation at frequency is given by:

$$\vartheta(\omega_r, \alpha) = \arctan \left[\frac{\omega_r^3 - \omega_n^2(1-4\zeta_n^2)\omega_r - 2\zeta_n \alpha_r \omega_n^2 \omega_r}{(\omega_n^2 - \omega_r^2)(2\zeta_n \omega_n - \alpha_r \omega_r) + 2\omega_r^2 \zeta_r \omega_r} \right] \tag{3}$$

The SMA method, as outlined in Ref. [16], defines the modal appropriation condition as $\vartheta(\omega_r, \alpha) = 0$. This criterion enables the estimation of the natural frequency and the damping ratio by finding the frequency ω_r that satisfies the appropriation condition. Specifically:

$$\vartheta(\omega_r, \alpha_r) = 0 \quad \Leftrightarrow \quad \begin{cases} \omega_r = \omega_n, \\ \alpha_r = 2\zeta_n \end{cases} \tag{4}$$

The complete r-th set of natural frequencies and damping ratios can be fully determined by applying the SMA modal appropriation condition to each n-th collection of filtered output response signals.
Once the natural frequencies are determined, under the assumption of a white noise excitation, it can be observed that the Power Spectral Density (PSD) of the input excitation is frequency independent and remains constant across the entire frequency band of the excitation. The ij-th element of the PSD matrix is given by:

$$G_{y_i,y_j}(\omega) = \sum_{k=1}^{N_{modes}} \frac{d_k \phi_i^{(k)} \phi_j^{(k)T}}{j\omega - \lambda_k} + \frac{d_k^* \phi_i^{(k)} \phi_j^{(k)H}}{j\omega - \lambda_k^*} \tag{5}$$

It can be demonstrated that, around a generic natural frequency w_{np}, the phase of the PSD approaches zero, while its real part exhibits either a maximum or a minimum. Using this relationship, the shape of the mode ϕ_i can be expressed as a function proportional to the real part of the corresponding diagonal term of the PSD Ref. [19]:

$$\phi_i^{(p)} = \frac{j2\zeta_{np}\omega_{np}^2}{d_p \phi_i^{(p)}} Re\left[G_{y_i,y_i}(\omega_{np})\right] \tag{6}$$

2.2. Proposed innovation

To further extend the applicability of the SMA method, which has proven effective in handling multi-degree-of-freedom systems, the proposed enhancements are introduced in this section to improve its performance in the case of closely spaced modes.
The fundamental assumption of the SMA method is that the system exhibits well-separated, uncoupled modes, ensuring a unique modal appropriation condition for each mode. The proposed approach, inspired by the Frequency Domain Decomposition (FDD) method, involves decomposing the system's N×N PSD matrix using Singular Value Decomposition (SVD).
The use of singular values serves three main purposes by calculating the singular values and the singular vectors. First, it provides an initial estimate of the system's natural frequencies. Second, it defines the frequency bandwidth within which the system can be considered a Single Degree of Freedom (SDOF) system, based on a threshold set for the Modal Assurance Criterion (MAC).
Since the MAC is computed between the singular vector ϕ_i and the frequency line near the peak represented by ϕ_{i-1}, it provides a measure of the similarity between these two vectors. In practice, if the MAC value remains above a predetermined threshold, it confirms that the response is dictates by a unique proper mode.
In this case, the system's dynamic response is governed by a single damped harmonic component, characteristic of SDOF behavior.
Third, this approach allows for the extraction of N-PSDs, each corresponding to a decoupled single harmonic oscillator. The SMA method, detailed in Section 2.1., is then applied to the decoupled PSDs. The new version of the SMA algorithm will henceforth be referred to as SDMA (Singular Decomposition Modal Appropriation).

3. DEVELOPED ALGORITHM

The algorithm, outlined in Fig. 1, starts by analyzing time response series obtained from measurements of the structure's operational response using sensors placed at different locations. This analysis is performed to estimate the Power Spectral Densities (PSDs), with one PSD computed for each output channel. This step facilitates signal pre-processing through the application of windowing functions. The pre-processed signal is then decomposed using Singular Value Decomposition (SVD).
In the left branch of Fig. 1, this decomposition, combined with the establishment of the MAC threshold, is used to define the bandwidth in which a system peak can be identified. The driving frequency, ω_r, is varied within this bandwidth at a spacing equal to the frequency resolution of the acquisition data to

verify the appropriation condition with a proper accuracy on the estimate.
The right branch of Fig. 1 describes the use of Singular Value Decomposition to transform the PSD matrix into a diagonal form, where each element corresponds to a simple harmonic oscillator. The rotating and stretching parameter α, constrained within a specific interval to avoid spurious modes, is then applied to each PSD. The modified PSD is subsequently convolved with a sine function, enabling the estimation of modal parameters through the appropriation condition.

4. NUMERICAL ANALYSIS

To evaluate the robustness and accuracy of the proposed algorithm, as well as its innovative aspects, numerically generated data is used to validate its reliability. The primary objective of this analysis is to determine whether the algorithm can accurately distinguish two natural modes as their separation distance decreases. Moreover, a robustness assessment is conducted to evaluate the method's sensitivity to noise. Keeping the system's modal properties fixed, the noise level in the response is progressively increased, and the resulting variations in the estimated natural frequencies and modal damping are analyzed.
To generate the numerical dataset, several systems, characterized by having two degrees of freedom, are synthesized in a modal basis, allowing the computation of the system's response to a random excitation input, thereby generating the time histories.
The consistency of the method is evaluated by varying the distance between the poles, according to the following criterion: the first natural frequency is held constant, while the second one is progressively reduced, halving the separation distance between the two adjacent poles at each step. This process challenges the underlying assumption of a single-degree-of-freedom behavior, which represents the foundation of the method.
In each generated system, the modal mass is fixed at 1 kg, and the first modal stiffness is chosen to ensure that the first natural frequency is exactly 10 Hz. The second modal stiffness is adjusted at each step to achieve the desired second frequency value. The modal damping is set to ensure a damping ratio of 0.03 for the first mode and approximately 0.0015 for the second. Notably, the random input time vector is generated once and applied consistently across all system configurations.
The identification of the modal parameters, natural frequency and damping ratio, is performed for each mode once the appropriation condition is met (see Eq. 4 for further details). Fig. 2 presents a plot of the logarithm of the phase (z-axis) as a function of the driving frequency ω_r(y-axis) and the rotation parameter α (x-axis) for the first mode which has constant natural frequency and modal damping for all the system in the dataset. As observed, when the phase approaches zero, its logarithm tends to $-\infty$. This behavior is visually represented by the negative spike in the logarithm of the phase, which identify the pair of parameters (ω_r,α) satisfying the appropriation condition.
Finally, the estimated modal parameters are compared with the exact numerical values, which serve as reference data. Table 1 presents a comparison of the estimated and theoretical natural frequencies and damping ratios for five distinct two-degree-of-freedom (2-DOF) systems, using both the standard SMA method and the SDMA (Singular Decomposition Modal Appropriation). In the table, d_{f_n} represents the distance between the two closely spaced poles, while $\epsilon_{f_{n_i}}$ and $\epsilon_{\zeta_{n_i}}$ denote the relative percentage error in the estimation of the modal parameters, computed as $\frac{|a_n^{NUM} - a_n^{EST}|}{a_n^{NUM}}$ where a_n^{NUM} represents the target value for both the natural frequency and damping ratio, and a_n^{EST} is the estimated value for the corresponding parameter.
As observed in table 1, the two natural frequencies are estimated with minimal error for the algorithm with the proposed innovation, even when the two peaks are very close. In contrast, the classic method is no longer able to distinguish two modes when the poles are spaced less than 4 Hz. Similarly, the damping ratio is generally well estimated using the SDMA algorithm, except for the second mode of the fourth system, where the mode spacing is 1 Hz.
Furthermore, the sensitivity of the algorithm to noise is evaluated by introducing additive Gaussian white noise to the response of each degree of freedom in the system. The analysis presented in table 2 considers

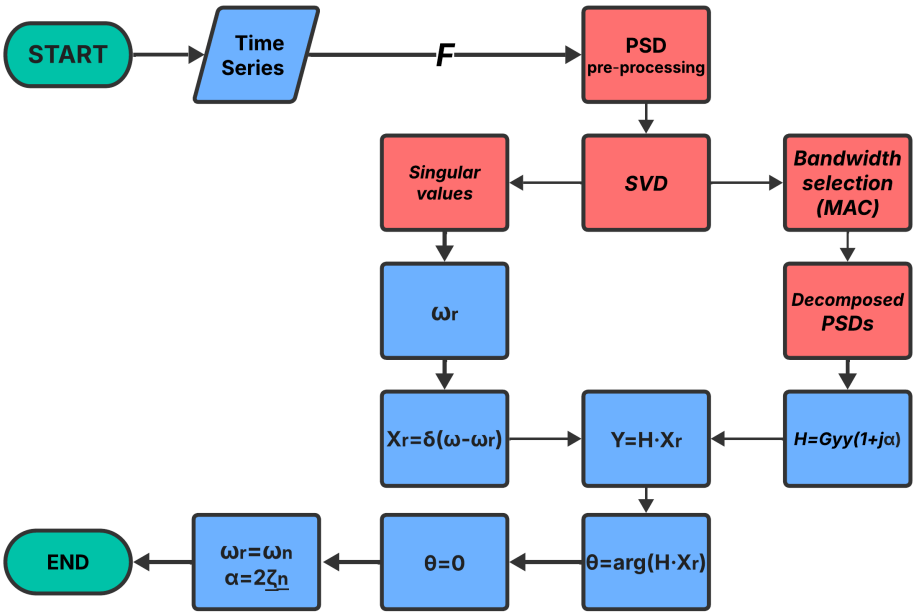

Figure 1: A flowchart of the developed SDMA algorithm is provided, with multiple boxes to represent the various steps. The proposed innovations are highlighted within red boxes, while the standard SMA algorithm steps are enclosed in blue boxes.

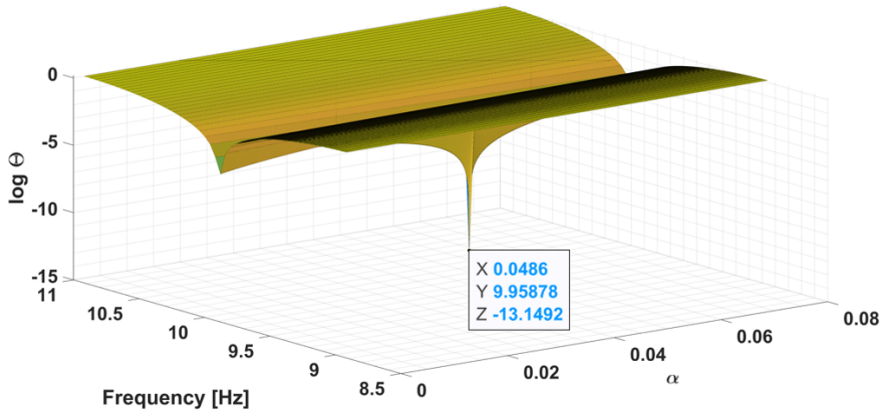

Figure 2: Representation of the appropriation condition: the logarithm of the phase shift approaches $-\infty$ as $\omega_n = \omega_r$ and $\alpha = 2\zeta_n$for the first mode, which remains invariant across all numerically generated two-degree-of-freedom systems.

the first two-degree-of-freedom system from table 1, which has the largest modal spacing, and progressively increases the noise-to-signal ratio by approximately 5% at each step. As shown, the estimation of modal frequencies remains unaffected by noise, demonstrating the robustness of the method to noisy data. In contrast, modal damping values are significantly influenced as noise levels increase.

Table 1: Comparison of Theoretical and Estimated Natural Frequencies and Damping Ratios for Five 2-DOF Systems with Varying Modal Spacings using both the standard SMA algorithm and the innovative SDMA one.

	Mode n°1				Mode n°2			
	$\epsilon_{f_{n1}}$		$\epsilon_{\zeta_{n1}}$		$\epsilon_{f_{n2}}$		$\epsilon_{\zeta_{n2}}$	
$d_{f_n}[Hz]$	SDMA	SMA	SDMA	SMA	SDMA	SMA	SDMA	SMA
8	0.41	0.10	19.0	46.7	0.01	0.44	17.7	186.7
4	0.01	0.80	52.8	26.7	0.01	0.57	67.3	53.3
2	0.41	1.60	61.2	20.0	0.01	N.A.	28.0	N.A.
1	0.41	N.A.	62.8	N.A.	0.71	0.36	159.7	146.7
0.5	0.41	N.A.	1.7	N.A.	0.18	0.95	10.0	80.0

5. APPLICATION TO A FLEXIBLE WING MODEL: PAZY-WING WIND TEST CASE

The developed algorithm is subsequently applied to a real test case that is the self-assembled model of the Pazy wing benchmark. This highly flexible wing was designed to provide experimental aeroelastic data for a structure experiencing large displacements, with the objective of validating numerical predictions for such geometric nonlinear test cases, Ref. [20].

The wing was manifactured at the Structural Dynamics Laboratory of the Department of Mechanical and Aerospace Engineering (DIMA) at the University of Rome La Sapienza. It consists of an aluminum spar, which serves as the primary structural component of the model, with 3D-printed ABS (Acrylonitrile Butadiene Styrene) ribs evenly spaced along the span of the longeron. The structure is wrapped in a heat-shrink film, which provides its aerodynamic characteristics.

To characterize the aeroelastic properties of the system, eight accelerometers are mounted on the wing, four at the trailing edge and four at the leading edge, distributed along the span of the aluminum spar.

The progressive assembly of the pazy wing is shown in Fig. 3, starting from the raw components, Fig. 3a, the sensors configuration, Fig. 3b, and the final assembly, Fig. 3c.

Several wind tunnel tests have been conducted over time at DIMA, varying the angle of attack, velocity,

Table 2: Impact of Additive White Gaussian Noise on Modal Frequency and Damping Estimation.

	Mode n°1		Mode n°2	
SNR	f_1	ζ_1	f_2	ζ_2
$+\infty$	9.96	0.0243	17.99	0.0153
13.01	9.96	0.0306	17.99	0.0265
10.00	9.96	0.0185	18.04	0.0295
8.24	9.96	0.0384	17.96	0.0279
6.99	9.96	0.0237	17.99	0.0154

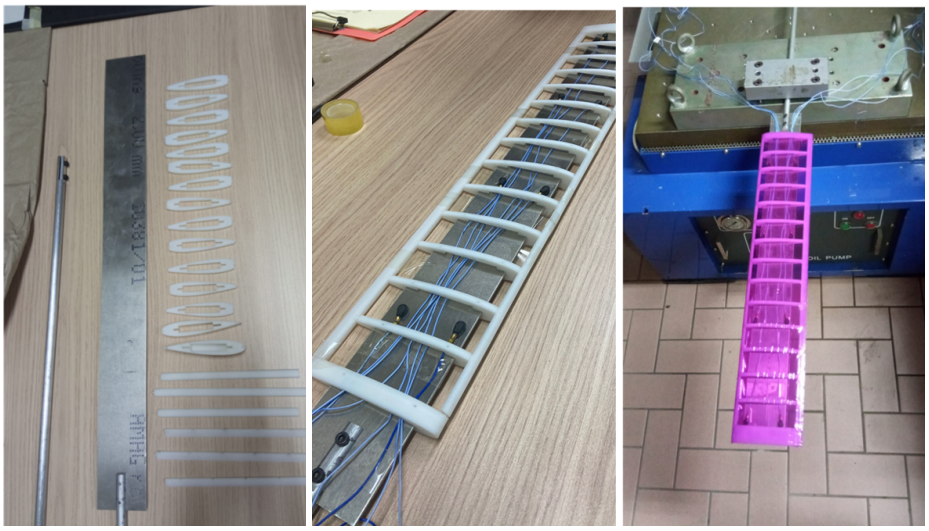

(a) **(b)** **(c)**

Figure 3: a: items, details of the rods, spar, ribs, leading and trailing edge; b: sensors configuration; c: assembly.

and boundary conditions. In this paper, the results focus on the vertical clamped configuration of the Pazy wing test, specifically for the angle of attack of 10° and at wind speed ranging from 5 to 34 $\frac{m}{s}$. Figure 4b shows the appropriation condition achieved for the third mode at a velocity of 5 $\frac{m}{s}$.

One way to represent the evolution of the modal parameters as the flow velocity changes is by illustrating the real and imaginary parts of the poles in a parametric diagram. The stable poles are located in the negative real part of the complex plane, which is justified by the negative exponent of the time-impulsive response function, leading to an exponential decay of the system's response.

The experimental root locus, obtained by post-processing the data with the SMA algorithm for each velocity, for the Pazy wing at an angle of attack of 10° is presented in figure 5. The modes are labeled with colored boxes indicating whether they are torsional, pure bending, or torsional-bending modes. The velocities are indicated in the figure using black text labels corresponding to each data point. It can be observed that the second bending mode coalesces with the first torsional mode, which, according to the current literature, is considered the primary driver of the flutter phenomenon. The SMA method provides the opportunity to identify a trend in the damping ratio that is representative of the physical behavior of the model, as confirmed by other more consolidated operational modal analysis methods, Ref. [8–10].

The evolving mode shapes, specifically the second bending and first torsional modes, estimated as described in Section 2.1., are shown in Figs. 6a and 6b at wind velocities of 0, 15, 27, and 34 $\frac{m}{s}$. The mode shapes, depicted in orange, oscillate around the system's equilibrium configuration (shown in gray) at the respective wind velocities, indicated by the bold numbers in the nearest boxes to each mode shape. The deformed shape is obtained by measuring the tip displacement using a photogrammetric technique and deriving the deformation along the span-wise direction, based on the extension of Euler-Bernoulli beam theory to the nonlinear geometric case. The mode is then applied to the configuration by first computing the local normal direction to the deformed shape and subsequently applying the modal displacement along the mentioned direction.

By examining Fig. 6a and 6b, the coalescence of the torsional and bending modes at high flow velocities becomes evident. This coupling is influenced by both the static deflection and the dynamic pressure acting on the wing. Notably, the bending mode transitions into a torsional mode, while the torsional mode transforms into a pure bending mode.

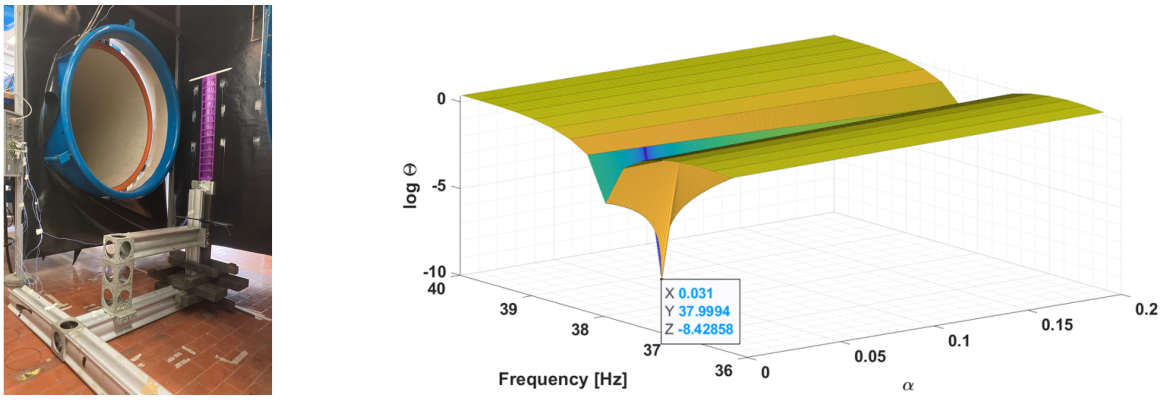

(a) **(b)**

Figure 4: (a) Experimental setup: vertical clamped condition of the Pazy Wing in the wind tunnel, (b)Representation of the appropriation condition: the phase shift approaches zero as $\omega_n = \omega_r$ and $\alpha = 2\zeta_n$.

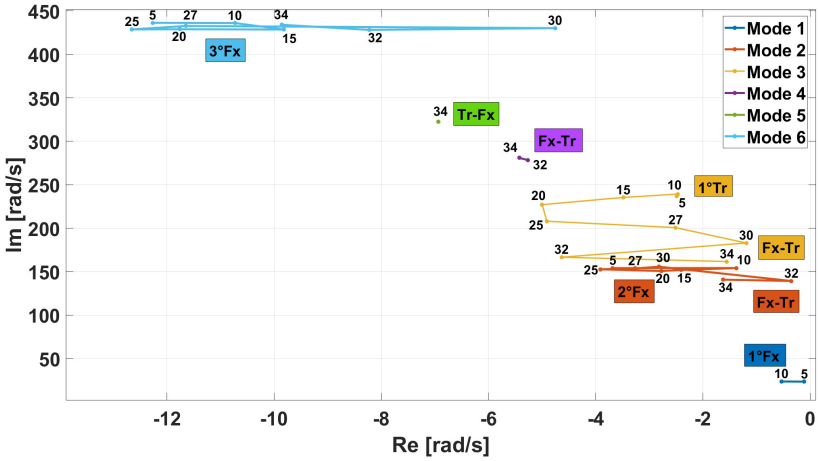

Figure 5: Root locus of the pazy wing at angle of attack equal to $10°$.

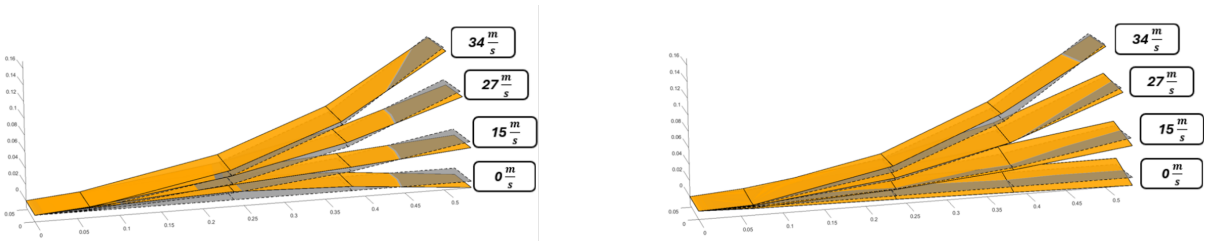

(a) **(b)**

Figure 6: (a) Evolution of the 2^{nd} bending mode to the 1^{st} torsional mode as the velocity goes from 0 to 34 $\frac{m}{s}$, (b) Evolution of the 1^{st} torsional mode to the 2^{nd} bending mode as the velocity goes from 0 to 34 $\frac{m}{s}$.

6. CONCLUDING REMARKS

In this work, a dynamic characterization of a flexible wing wind tunnel model using the Stochastic Modal Appropriation (SMA) technique is proposed. The resulting algorithm has been assessed with numerically generated data for a two-DOF mass-spring-damper system with fixed properties and subsequently applied to the real test case of the Pazy wing benchmark. The algorithm demonstrates robustness in both applications, successfully capturing the flutter mechanism of the Pazy wing as reported in the literature. However, further investigation is required into modal damping in order to refine the results and fully characterise the aeroelastic behaviour. Indeed, while the SMA method tends to return higher values of damping coefficients compared to MDOF approaches, it accurately captures the overall trends, thereby reflecting the dynamic response behaviour with sufficient reliability.

REFERENCES

[1] Ariel Drachinsky and Daniella E Raveh. Nonlinear aeroelastic analysis of highly flexible wings using the modal rotation method. *AIAA Journal*, 60(5):3122–3134, 2022.

[2] Frederico Afonso, José Vale, Éder Oliveira, Fernando Lau, and Afzal Suleman. A review on nonlinear aeroelasticity of high aspect-ratio wings. *Progress in Aerospace Sciences*, 89:40–57, 2017.

[3] Weihua Su and Carlos ES Cesnik. Dynamic response of highly flexible flying wings. *AIAA journal*, 49(2):324–339, 2011.

[4] Alvaro Cea and Rafael Palacios. Nonlinear modal aeroelastic analysis from large industrial-scale models. In *AIAA Scitech 2019 Forum*, page 0208, 2019.

[5] Deman Tang and Earl H Dowell. Experimental and theoretical study on aeroelastic response of high-aspect-ratio wings. *AIAA journal*, 39(8):1430–1441, 2001.

[6] Pawel Chwalowski. Aeroelastic Prediction Workshop 3 Website. `https://nescacademy.nasa.gov/workshops/AePW3/public/`, 2016. [Online; accessed 20.05.2024].

[7] Or Avin, Daniella E Raveh, Ariel Drachinsky, Yaron Ben-Shmuel, and Moshe Tur. Experimental aeroelastic benchmark of a very flexible wing. *AIAA Journal*, 60(3):1745–1768, 2022.

[8] Marcello Righi, Giuliano Coppotelli, Gabriele Immordino, Andrea Da Ronch, Ludovica Onofri, Roberto Sbarra, and Giampaolo Romano. Experimental characterization of flutter and lco of a very flexible wing. In *AIAA SCITECH 2024 Forum*, page 0831, 2024.

[9] Giuliano Coppotelli, Roberto Giovanni Sbarra, Ludovica Onofri, Marcello Righi, et al. Experimental investigation of a highly flexible wing. In *International Forum on Aeroelasticity and Structural Dynamics*, pages 1–18, 2024.

[10] Giuliano Coppotelli, Roberto G Sbarra, Ludovica Onofri, Marcello Righi, Gabriele Immordino, and Andrea Da Ronch. Experimental characterization of the flutter behavior of a very flexible wing. In *AIAA SCITECH 2025 Forum*, page 1019, 2025.

[11] Rune Brincker, Lingmi Zhang, and Palle Andersen. Modal identification from ambient responses using frequency domain decomposition. In *IMAC 18: Proceedings of the International Modal Analysis Conference (IMAC), San Antonio, Texas, USA, February 7-10, 2000*, pages 625–630, 2000.

[12] Alessandro Agneni, Luigi Balis Crema, and Giuliano Coppotelli. Output-only analysis of structures with closely spaced poles. *Mechanical systems and signal processing*, 24(5):1240–1249, 2010.

[13] Peter Van Overschee and BL0888 De Moor. *Subspace identification for linear systems: Theory—Implementation—Applications*. Springer Science & Business Media, 2012.

[14] Samir R Ibrahim and Richard S Pappa. Large modal survey testing using the ibrahim time domain identification technique. *Journal of Spacecraft and Rockets*, 19(5):459–465, 1982.

[15] R. Sbarra and Giuliano Coppotelli. Dbscan-based approach for the automatic estimate of the modal parameters. In Carlo Rainieri, Carmelo Gentile, and Manuel Aenlle López, editors, *Proceedings of the 10th International Operational Modal Analysis Conference (IOMAC 2024)*, pages 618–630, Cham, 2024. Springer Nature Switzerland. ISBN 978-3-031-61421-7.

[16] M. Abdelghani and M. I. Friswell. Stochastic modal appropriation (sma). In Michael Mains and Brandon J. Dilworth, editors, *Topics in Modal Analysis & Testing, Volume 9*, pages 1–4, Cham, 2019. Springer International Publishing.

[17] Maher Abdelghani. Physical only modes identification using the stochastic modal appropriation algorithm. In Abdo Abou Jaoudé, editor, *The Monte Carlo Methods*, chapter 8. IntechOpen, Rijeka, 2022. doi: 10.5772/intechopen.101224. URL https://doi.org/10.5772/intechopen.101224.

[18] M Abdelghani and MI Friswell. Stochastic modal appropriation (sma). In *Topics in Modal Analysis & Testing, Volume 9: Proceedings of the 36th IMAC, A Conference and Exposition on Structural Dynamics 2018*, pages 1–4. Springer, 2019.

[19] Giuliano Coppotelli, Gabriele Muto, and Maher Abdelghani. Identification of modal parameters in rotating structures using stochastic modal appropriation (sma). *AIAA SCITECH 2023 Forum*, 2023. URL https://api.semanticscholar.org/CorpusID:256180834.

[20] Markus Ritter, Michael Fehrs, and Christoph Mertens. Aerodynamic and static coupling simulations of the pazy wing with transitional cfd for the third aeroelastic prediction workshop. In *AIAA Scitech 2023 Forum*, page 0762, 2023.